American Mineralogist, Volume 71, pages 1441–1454, 1986

Transformation mechanisms between single-chain silicates

Ross John Angel*
Department of Earth Sciences, University of Cambridge, Downing Street, Cambridge CB2 3EQ, England

Abstract

The single-chain silicate structures of clinopyroxene, bustamite, and pyroxenoids are compared. The possible types of transformations between these structures are then characterized in terms of the change in lattice type accompanying the structural transformation. Four types of transformation are shown to occur; these may be divided into two groups. Observations made by high-resolution transmission-electron microscopy on partially transformed samples show that the mechanism of transformation between clinopyroxene and the pyroxenoids is one of glide of line defects on {001} of pyroxenoid and on {11$\bar{1}$} of clinopyroxene. The structural reorganization associated with the passage of such a line defect shows that it is not truly a partial dislocation, but that various different displacements of atoms occur in the core of the defect.

Comparison of the structure of bustamite with that of the pyroxenoids shows that with the cell setting in which the latter possess a *C*-face-centered lattice, bustamite has a lattice that is best described as an interleaved complex of two *F* lattices. This indicates that the relative positioning of the silicate chains in bustamite is different from that in the pyroxenoids or clinopyroxene. Consequently, inversions in the solid state between bustamite and either clinopyroxene or pyroxenoid must proceed by mechanisms that carry out the inversions in two steps. Observations made by high-resolution transmission-electron microscopy on partially inverted samples indicate that the inversions from bustamite proceed by the propagation through the structure of line defects with Burgers vectors of ½[010] on the {102} planes ($A\bar{1}$ cell) which create a wollastonite-like intermediate structure. This intermediate structure subsequently inverts to either clinopyroxene or pyroxenoid. The initial stage of the inversions in the opposite direction is shown also to be the creation of this wollastonite-like structure, probably by the glide of line defects on the {001} planes of pyroxenoid or the {11$\bar{1}$} planes of clinopyroxene.

Introduction

There are three main structure types for single-chain silicates of formula $MSiO_3$ (M = Ca,Mn,Fe,Mg): clinopyroxene, pyroxenoid, and bustamite. They are distinguished by the different relative positioning of the chains in each structure, that is, by their lattice types. Transformations between these phases have been the subject of several single-crystal X-ray studies during which one phase is inverted to another by heating. These studies have shown that the inversions are topotactic and pseudomorphous (Dent-Glasser and Glasser, 1961; Morimoto et al., 1966; Aikawa, 1979). The relative orientations of reactant and product phases have been used by these workers to derive atomic-scale transformation mechanisms that involve the cooperative diffusion of cations. This derivation of atomic-scale mechanisms from the relative orientation of reactant and product phases in a transformation is clearly not satisfactory. And although the pyroxenoids have been the subject of many high-resolution transmission-electron microscopy (HRTEM) studies, there has yet to be an attempt to relate the observed faults to possible transformation mechanisms between the various structures. Indeed, since most of the high-resolution observations of pyroxenoids have been made on synthetic material, the observed faults are more likely growth features than the result of incipient phase transformation.

In this paper the three structure types of single-chain silicates are compared, and the structural reorganization associated with each possible transformation is described. After a review of the possible types of transformation mechanism, the results of a HRTEM study of a number of partially inverted chain silicates are presented. The combination of these unit-cell-scale observations with data previously available from X-ray studies is shown to be consistent with the suggestion of Angel et al. (1984) that such transformations may proceed by the propagation of line defects through the structure of the starting material.

Structures

The crystal structures of chain silicates may be described as the stacking together of tetrahedral and octahedral layers (e.g., Pannhorst, 1979). In the case of py-

* Present address: Geophysical Laboratory, Carnegie Institution of Washington, 2801 Upton Street, N.W., Washington, D.C. 20008, U.S.A.

0003–004X/86/1112–1441$02.00

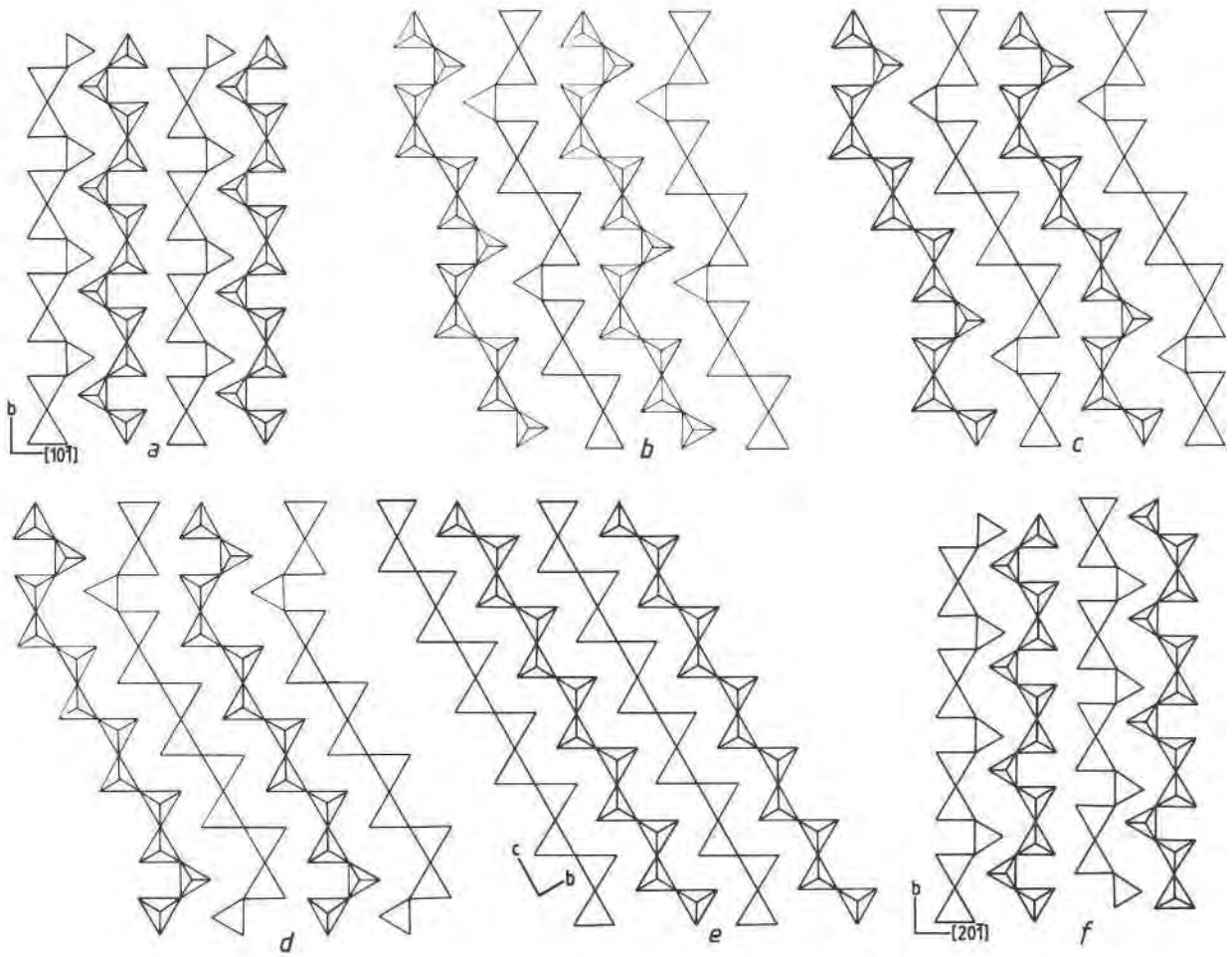

Fig. 1. Idealized chain configurations of pyroxenoids projected onto (100). (a) Wollastonite. (b) Rhodonite. (c) Pyroxmangite. (d) Ferrosilite III. (e) Clinopyroxene. (f) Bustamite.

roxenoids the oxygens coordinating these layers approximate a close-packed array; this plane is chosen to be (100). In this cell setting (due to Koto et al., 1976), the tetrahedral chains lie in the (100) planes and extend along the **c** axis. The **b** axis defines the relative displacements of adjacent chains within the (100) layers, and the lattice type defines the relative positions of chains in the adjacent (100) layers. The idealized chain configurations within (100) layers of the observed pyroxenoid structures are shown in Figures 1a–1d. Each chain repeat unit consists of a number of pyroxene-like pairs of tetrahedra, followed by three tetrahedra in a wollastonite-like configuration. Thus the pyroxenoid minerals have chain-length periodicities given by $p = 2n + 3$ (n integral): wollastonite (p = 3), rhodonite (p = 5), pyroxmangite and pyroxferroite (isostructural with $p = 7$), and ferrosilite III ($p = 9$). Mineral structures with periodicities greater than nine are not known, but such repeats have been observed as short sequences in partially disordered material.

Clinopyroxenes have often been described as pyroxenoids with formal periodicity of $p = \infty$, i.e., with a chain repeat unit with an infinite distance between consecutive wollastonite-like chain units. Unfortunately this has led, incorrectly, to the description of pyroxenoids as a structural series made up of pyroxene and wollastonite slabs (modules), clinopyroxene thus being composed of an infinite stack of pyroxene modules (e.g., Koto et al., 1976; Czank and Liebau, 1980).

Although within a single (100) layer the relative positioning of the tetrahedral chains in clinopyroxene and the pyroxene-like portions of the pyroxenoid chains is the same (Fig. 1), the relative position of the tetrahedral chains in adjacent (100) layers differs in clinopyroxene and the pyroxenoids (Fig. 2). In pyroxenoids the direction of the **b** axis is defined by the relative positions of the offset tetrahedra of the wollastonite-chain units, and consequently α increases with increasing chain periodicity from 99° in wollastonite to 114° in ferrosilite III (Koto et al., 1976). In order to properly compare the pyroxene structure with that of the pyroxenoids, α of the clinopyroxene cell should be increased to 120° by a new choice of **b** axis, as indicated in Figure 2b. With this cell orientation the

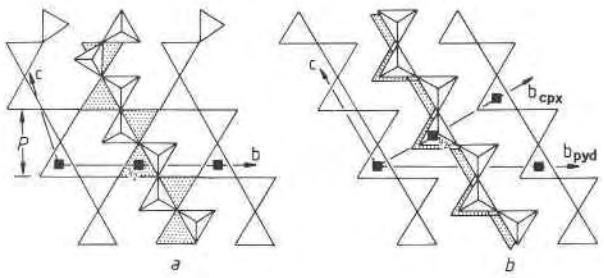

Fig. 2. Tetrahedral chains in consecutive (100) layers in (a) pyroxenoid and (b) clinopyroxene. The shaded chains consist of apex-down tetrahedra related to the left-hand chain by the *C*-lattice vectors in each structure. Note that when clinopyroxene is described on axes parallel to those of the pyroxenoids, it has an *I* lattice.

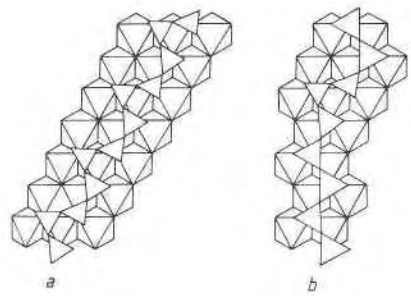

Fig. 3. Single tetrahedral chains with associated octahedral bands in (a) wollastonite and (b) a long-period pyroxenoid. Note the association of the three-site-wide portions of octahedral band with the wollastonite-like units in the tetrahedral chains.

lattice of clinopyroxene is body centered. Since the lattice type controls the relative positions of the tetrahedral chains, it is clear that the chains in clinopyroxene are arranged differently from those in the pyroxene-like modules of the pyroxenoids. If a structure was composed entirely of these modules, alternate (100) layers of tetrahedral chains would have to be translated by ½[001] in order to reproduce the observed clinopyroxene structure. This argument also applies to the $P2_1/c$ clinopyroxenes since these have the same general positioning of silicate chains as the $C2/c$ structures; the displacive transformation between the two structures, when it occurs, consists mainly of tetrahedral rotation.

Interleaved with the (100) tetrahedral layers are layers of large cation sites that are generally of octahedral coordination. The cation sites in pyroxenoids form bands that run parallel to the tetrahedral chains, the bands being two sites wide when associated with the pyroxene-like portions of the tetrahedral chains and three sites wide when associated with the wollastonite-like chain units (Fig. 3). The structures of the pyroxenoid minerals may therefore be considered as being formed from the stacking together of two types of structure module. The wollastonite module, denoted W, is a one-unit-cell-thick layer of wollastonite cut parallel to (001), i.e., approximately perpendicular to the chain extension direction. The pyroxene-like module, P, may either be considered to be the residual structure left after removal of the W modules from rhodonite, or be derived from clinopyroxene by the glide of alternate octahedral + tetrahedral layers by ½[001]—one-half of the chain repeat distance. Thus the P module is also a layer parallel to (001) of pyroxenoid, but contains a pair of tetrahedra from each silicate chain. The observed stacking sequences are

Wollastonite	⟨W⟩	$p = 3$
Rhodonite	⟨WP⟩	$p = 5$
Pyroxmangite	⟨WPP⟩	$p = 7$
Ferrosilite III	⟨WPPP⟩	$p = 9$.

The cation sites associated with the W modules are generally able to accommodate larger cations than those in the P modules, because of the greater degree of rotation possible for the associated wollastonite tetrahedral-chain units. The various stability fields of the stacking sequences composing the pyroxenoid structures are thus strongly dependent upon the relative sizes and proportions of octahedral cations. As the average cation size is increased, those phases with a larger proportion of wollastonite-type slabs are stabilized with respect to those with less. Thus, in general, the chain-length periodicity of the stable pyroxenoid phase increases with increasing pressure, decreasing temperature, and decreasing average radius of nontetrahedral cations (Simons and Woermann, 1982). Consequently the chain periodicity of a structure may change in response to a change in one of these variables, giving rise to transformations between pyroxenoids, and between pyroxenoid and clinopyroxene. The various transformations are best characterized by the change in lattice type that accompanies the change in structure:

Pyroxenoid	→ Pyroxenoid	$C \rightarrow C$
Clinopyroxene	→ Pyroxenoid	$I \rightarrow C$
Pyroxenoid	→ Bustamite	$C \rightarrow$ "*F*-complex"
Clinopyroxene	→ Bustamite	$I \rightarrow$ "*F*-complex."

Complications are introduced into possible transformation behavior by the fact that the bustamite structure, which has a chain periodicity of three, is more stable over much of the $(Ca,Fe,Mn)SiO_3$ system than the wollastonite structure to which it is closely related. The structure of bustamite, when described on axes that parallel those of the pyroxenoid $C\bar{1}$ cell settings, does not possess a simple lattice type. Koto et al. (1976) described the resultant lattice as a complex of two interleaved *F*-lattices.

Transformation mechanisms

In most of the oriented transformations between silicate minerals, the oxygen atoms tend to preserve their positions when possible, whereas the Si and other cations are redistributed within this anion framework (Taylor, 1960). The transformations considered here are all between structures that possess approximately the same oxygen

packing, so that cation displacement is the only major structural change associated with each transformation. The two types of mechanisms proposed for these transformations achieve these changes in different ways.

Dent-Glasser and Glasser (1961) described the experimental inversion of rhodonite to what they termed "wollastonite." The mechanism proposed by Dent-Glasser and Glasser (1961) for this transformation requires the movement of Si atoms, with minor displacements of the oxygen atoms. A similar mechanism of cooperative cation diffusion was proposed by Morimoto et al. (1966) for the inversion of johannsenite (a Ca-Mn clinopyroxene isotypic with diopside) to bustamite in which the relative orientation of johannsenite and product bustamite is controlled by the preservation of the oxygen layers coordinating "dense-zones" of cations common to both structures. This type of mechanism has also been proposed for the transformation of rhodonite to bustamite (Morimoto et al., 1966) and for that between rhodonite and pyroxmangite (Aikawa, 1979).

The second type of mechanism proposed for these transformations employs the passage of partial dislocations through a structure to create an atomic configuration that locally resembles that of the product phase. Dislocations were originally proposed as a microscopic explanation of the process of slip in metals. The Burgers vector of a dislocation is defined as the displacement created by the dislocation between slipped and unslipped material. It is thus a measure of the displacement of all the atoms of the structure caused by the passage of one dislocation. But in the case of more complex materials such as the silicates studied here, the process of shear by a dislocation creates energetically unfavorable environments for some atoms, and these undergo a further redistribution into more favorable sites (synchroshear; Kronberg, 1957). The passage of line defects has already been shown to be the mechanism by which polytypically disordered bustamite eliminates stacking mistakes (Angel, 1985). And the observation of stacking faults in spinel from the Peace River meteorite (Price et al., 1982) is consistent with the transformations between spinel and spinelloids [specifically the beta phase of $(Fe,Mg)_2SiO_4$ in this case] proceeding by the passage of line defects. Electron microscopy of similar shocked material from the Tenham chondritic meteorite (Putnis and Price, 1979) and of synthetic material (Lacam et al., 1980) supports the proposal by Poirier (1981) that the olivine-to-spinel inversion also proceeds under certain conditions by a shear mechanism.

In the following sections the four types of transformation (as characterized by the change in lattice type) between the single-chain silicates are examined in more detail. Evidence from HRTEM observations of partially inverted samples suggests that these transformations proceed by the passage of line defects. The orientational relationship between the phases created by this mechanism is approximately the same as that predicted by the dense-zone theory.

Pyroxenoid to pyroxenoid ($C \rightarrow C$)

Aikawa (1979) studied the inversion between pyroxmangite and rhodonite by single-crystal X-ray techniques. He proposed that the inversion proceeded by the cooperative diffusion of two-fifths of the Si and other cations into sites that are vacant in the pyroxmangite structure, and that the relative orientation of the reactant and produce phases is controlled by the preservation of the oxygen layers coordinating "dense-zones" of cations common to both structures.

Angel et al. (1984) derived a possible shear mechanism primarily for the inversion of johannsenite to bustamite and then applied the same principles to inversions involving the pyroxenoid structures. It should be pointed out that, as a consequence of a misunderstanding of the precise structural relationship between clinopyroxene and the pyroxenoids, the Burgers vectors derived in the appendix to Angel et al. (1984) for the pyroxenoid-to-pyroxenoid inversions are not vectors of the oxygen sublattices of the structures and are therefore incorrect. They are now derived correctly for the idealized structures.

The periodicity of pyroxenoids is defined by the frequency with which the wollastonite modules appear in the stacking sequence. Each of these modules contributes one offset tetrahedron to each tetrahedral chain (Fig. 1), and the principle of the derivation of the shear mechanism is to create one such offset tetrahedron in a pyroxene-like portion of one chain. As described in Angel et al. (1984), this tetrahedron is generated by the movement of a tetrahedral chain into a position offset from that related by the C-lattice vector. The Burgers vector of the shear required for such a movement is the sum of the same C-lattice vector as for the clinopyroxene-to-bustamite inversion (Angel et al., 1984), $\frac{1}{2}[1\bar{1}0]$, and the equivalent of the offset vector, $\frac{1}{4}[0\bar{1}\bar{1}]_{cpx}$. On axes parallel to those of the pyroxenoids (Fig. 2b) this offset vector in clinopyroxene becomes $\frac{1}{4}[0\bar{1}\bar{2}]$. The formal description of this offset vector will vary not only from pyroxenoid to pyroxenoid because of differences in chain periodicity, but also within a pyroxenoid because of the deviations of the tetrahedral chains away from the idealized structures considered here. Alternatively, these deviations may be considered to be accommodated by the structural relaxation that follows the shear. In the idealized structures the offset may be rewritten in terms of the chain periodicity p as $\frac{1}{4}[0\bar{1}\bar{4}/p]$, giving the Burgers vectors of the shears in each structure type as

Wollastonite	$\frac{1}{4}[2\ \bar{3}\ \bar{4}/3]$	(203)
Rhodonite	$\frac{1}{4}[2\ \bar{3}\ \bar{4}/5]$	(205)
Pyroxmangite	$\frac{1}{4}[2\ \bar{3}\ \bar{4}/7]$	(207)
Ferrosilite III	$\frac{1}{4}[2\ \bar{3}\ \bar{4}/9]$	(209).

The slip planes are derived by a similar transformation of the slip plane in clinopyroxene, which becomes {101} on the I-centered cell, and by the constraint that the Bur-

gers vector of a glissile dislocation must lie in the slip plane. Note that the slip planes are slightly inclined to the (001) interfaces of the W and P modules of which the pyroxenoids are composed, and therefore shear on these planes would cut across the modules and convert one module type to the other. Calculation shows that if rhodonite and pyroxmangite are intergrown with these slip planes and with their **b** axes parallel, the relative orientation of the two phases is the same as that predicted by the dense-zone preservation theory.

Observations

The easiest transformation to study is that between rhodonite and pyroxmangite because of the low temperature at which the inversion takes place. Aikawa (1979) carried out annealing experiments to invert natural pyroxmangites to rhodonite. Despite undergoing partial oxidation of the Mn^{2+} and Fe^{2+} in the pyroxmangite, the product rhodonite showed the orientation relationship to the pyroxmangite predicted by the dense-zone theory of Morimoto et al. (1966). Although Aikawa (1979, 1984) was able to demonstrate that many natural intergrowths of pyroxmangite and rhodonite also exhibit this orientation relationship, Ried and Korekawa (1980) reported fine-scale intergrowths and chain-periodicity faults in pyroxenoids that are oriented slightly differently. Unfortunately the other HRTEM studies of pyroxenoids reported in the literature (Czank and Liebau, 1980; Jefferson et al., 1980; Jefferson and Pugh, 1981) do not give sufficient details for the precise orientation relationships to be ascertained. These chain-periodicity faults and intergrowths generally show very little strain, but Ried and Korekawa (1980) noted that they are often terminated by dislocations within the crystal, which suggested that transformations may proceed by the passage of partial dislocations.

In order to ascertain the type of mechanism operative during pyroxenoid-to-pyroxenoid transformations, a series of inversion experiments was carried out with synthetic material of $MnSiO_3$ composition. A glass was prepared from a mixture of silica and manganese sulfate by the same method as described in Angel (1984). A series of hydrothermal devitrification runs was then carried out, which produced samples consisting of various mixtures of rhodonite and pyroxmangite, the starting material for the inversion experiments coming from a two-week run at 1.5 kbar and 650°C. Although these conditions are within the rhodonite stability field, HRTEM of material from this run showed that it contained an appreciable proportion of pyroxmangite and had a very low density of stacking faults. This material was then annealed under pure Ar (to prevent oxidation) at higher temperatures to invert the pyroxmangite to rhodonite.

Observations made on the products of several annealing runs show that the proportion of rhodonite increases relative to pyroxmangite with increased annealing time within the rhodonite stability field. The residual pyroxmangite also appears to have an increased density of chain periodicity faults, especially of those with the rhodonite structure, but no direct evidence of the mechanism of formation of these faults was found. However, a possible mechanism is suggested by micrographs of a rhodonite produced in a longer annealing run. Figure 4a shows a number of line defects within a rhodonite grain that run parallel to the incident electron beam (along $[1\bar{1}0]$) and that terminate the (001) chain-periodicity faults. An enlargement of an area of this micrograph is provided in Figure 4b, and the structural interpretation based upon image matching using the SHRLI (Simulation of High-Resolution Lattice Images) program (O'Keefe and Buseck, 1979) is drawn in Figure 4c. The rows of bright spots in the micrograph are associated with the wollastonite-like units within each tetrahedral chain, so that the periodicity faults consist of two W modules without an intervening P module, i.e., a short portion of two unit cells of wollastonite structure. For the $MnSiO_3$ composition, such a structure is not stable, and this sample appears to be in the process of eliminating such faults by the passage of line defects through the structure. At each defect it would appear that local atom displacements occur, possibly using the empty core of the line defect as a fast diffusion path. The concept of a Burgers vector of a shear is not strictly applicable to such a defect, but bearing in mind that the line of the defect is parallel to a *C*-lattice vector, the actual atomic reorganization may well be that which was described by the shear mechanism derived above. The only difference lies in the planes on which the defects travel through the structure; the slip plane of the shear mechanism was (205) in rhodonite, but is obviously (001) in the micrographs, while consideration of the structural rearrangement required at the defects of Figure 4 indicates that atom displacements with components normal to the (001) planes are necessary. Such atom rearrangements within the core of the line defect will also include the movement of the octahedral cations, which was previously assigned to the final mechanistic step of syncroshear after the passage of a partial dislocation.

Similar line defects were also observed in the products of the very short hydrothermal annealing runs of the $MnSiO_3$ glass, in which longer chain periodicities are being eliminated (Fig. 5). It therefore seems likely that the pyroxmangite-to-rhodonite inversion carried out in these experiments also proceeded by the passage of these line defects. This would account for the increasing density of chain-periodicity faults in the pyroxmangite, and if such defects nucleated at the wrong relative spacings, they would generate the WW-type (001) chain-periodicity faults being eliminated in Figure 4.

Clinopyroxene to pyroxenoid ($I \rightarrow C$)

The replacement of clinopyroxene by pyroxenoid was discussed at length by Angel et al. (1984), who proposed that the transformation mechanism was one of dislocation glide followed by cation synchroshear. The slip plane may be derived by considering which lattice plane of clino-

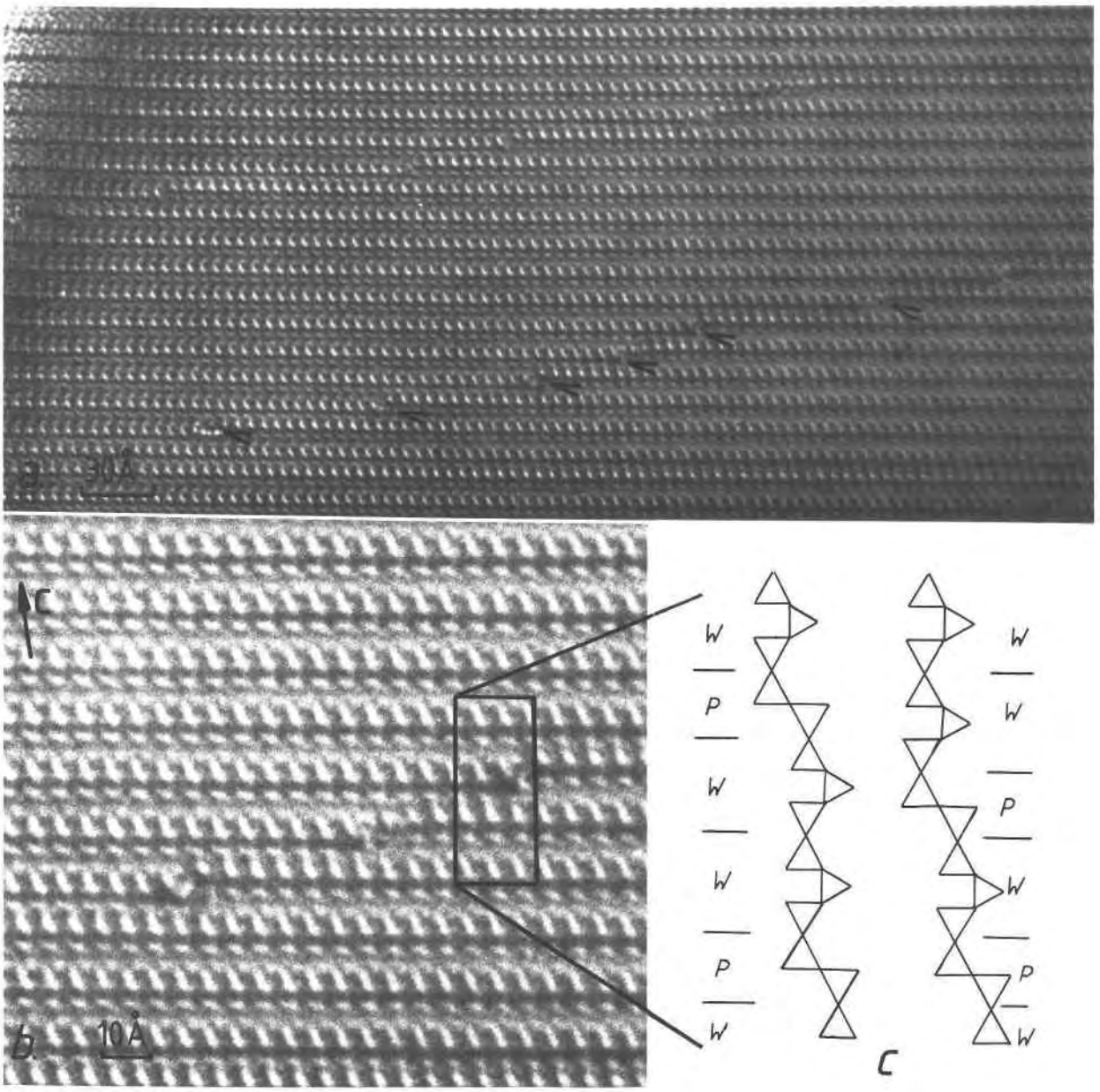

Fig. 4. Transformation of stacking sequences in rhodonite by line defects that run parallel to the incident direction of the electron beam, $[1\bar{1}0]$. (a) Note the "en echelon" arrangement of the line defects that lie on every (001) plane of the rhodonite. (b) Enlargement of a portion of the micrograph in (a), together with a structural interpretation (c). Note that interpretation of the structure in the core of the defect is not possible at this resolution.

pyroxene best matches that of (001) of pyroxenoids and has the same centering of lattice points. The latter condition ensures that the relative positioning of the chains in a pyroxenoid structure formed by the inversion of clinopyroxene is correct. Figure 6 shows that the $\{11\bar{1}\}$ planes of clinopyroxene fulfill these conditions, this being the slip plane of the mechanism proposed by Angel et al. (1984), the Burgers vectors of the dislocations being $\frac{1}{4}\langle 2\bar{3}\bar{1}\rangle$.

Intergrowths of clinopyroxene with various pyroxenoids have been reported in HRTEM studies of synthetic material. In a study of ferrosilite III, Czank and Simons (1983) found long periods of pyroxene-like structure intergrown with the pyroxenoid with $\{11\bar{1}\}_{cpx}$ parallel to $\{001\}_{pyd}$. A more detailed study of similar intergrowths by Ried (1984) confirmed the orientation relationship predicted by the proposed shear mechanism and showed that the displacement vector associated with the chain-periodicity faults in the clinopyroxene was $\frac{1}{4}\langle 011\rangle$. Since the addition of a C-lattice vector, $\frac{1}{2}[\bar{1}\bar{1}0]$, and $\frac{1}{4}[0\bar{1}\bar{1}]$ is equal

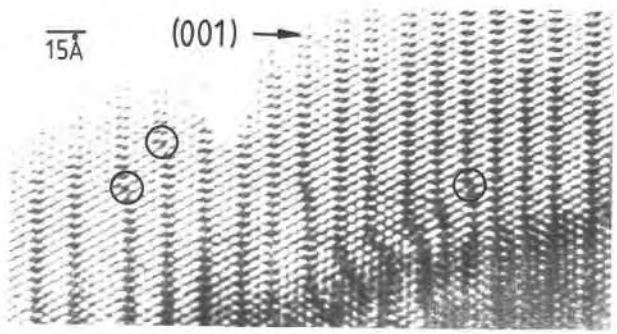

Fig. 5. Line defects (some circled) running parallel to [1$\bar{1}$0] in a disordered pyroxenoid.

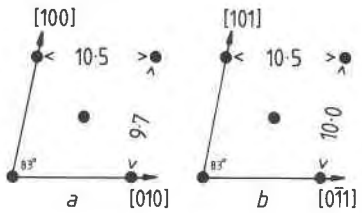

Fig. 6. (a) The (001) lattice section of a pyroxenoid: lattice parameters taken from pyroxmangite. (b) A {11$\bar{1}$} lattice section of johannsenite (clinopyroxene). Lattice spacings in ångströms are indicated.

to ¼[23$\bar{1}$], this also is consistent (see, for example, Amelinckx and Van Landuyt, 1976, p. 95) with the proposed mechanism. Even so, these observations were made on synthetic material in which the microstructures described are *growth* features, and do not necessarily constitute evidence for the transformation mechanism.

Veblen (1985) reported observations made by HRTEM on a natural johannsenite that clearly shows petrographic evidence of having undergone partial inversion to rhodonite. His observations of pyroxenoid lamellae parallel to the {11$\bar{1}$} planes of the clinopyroxene matrix are strong evidence in favor of the shear mechanism proposed by Angel et al. (1984). Similar chain-periodicity errors were observed occasionally in natural johannsenite (Fig. 7a) in which longer periodicities corresponding to {001} pyroxenoid spacings occur parallel to the {11$\bar{1}$} planes of the clinopyroxene matrix. Some of the material was experimentally annealed in a Mn solution below the temperature of inversion to bustamite in order to demonstrate that such microstructures are the product of a partially completed transformation. The increase in the Mn content of the structure has promoted the creation of extensive stacking disorder on {11$\bar{1}$} of the clinopyroxene matrix (Fig. 7c). The associated selected-area electron-diffraction pattern (Fig. 7b) shows maxima corresponding to wollastonite and rhodonite, together with diffuse streaks parallel to the (11$\bar{1}$) plane normal of the clinopyroxene. By contrast, diffraction patterns from clinopyroxene annealed in $CaCO_3$ solution show strong maxima from wollastonite alone (Fig. 7d), whereas the maxima corresponding to longer chain periodicities are very diffuse or absent. The orientation relationship observed in these samples is ⟨101⟩ of clinopyroxene parallel to ⟨100⟩ of pyroxenoid as expected from the matching of the two lattice types. The disorder is therefore characterized by short sequences of pyroxenoid mineral structures intergrown with clinopyroxene, with {001} of the pyroxenoids parallel to one of the {11$\bar{1}$} planes of the clinopyroxene.

BUSTAMITE TRANSFORMATIONS

As was the case for the $C \rightarrow C$ and $C \rightarrow I$ transformations discussed above, two types of mechanism have been proposed for the inversions of chain silicates to bustamite. Dent-Glasser and Glasser (1961) described the inversion of rhodonite upon heating, but because of their belief that the inversion product was wollastonite and not bustamite, their mechanism of cation diffusion partly generates the wollastonite structure (Prewitt and Peacor, 1964). Morimoto et al. (1966) also studied the inversion of various chain silicates to the bustamite structure. However, inconsistencies appear in the discussion given by Morimoto et al. (1966); the diagrams from which the dense-zone preservation theory is derived are all of wollastonite, rather than bustamite, while Figure 12b of their paper, which is labeled bustamite, is identical to Figure 15b, described as wollastonite. It would therefore appear that instead of producing bustamite, the transformation mechanisms proposed by Morimoto et al. for both the clinopyroxene-to-bustamite ($I \rightarrow F$-complex) and the rhodonite-to-bustamite ($C \rightarrow F$-complex) inversions produce (incorrectly) the wollastonite structure.

Because of the differences in lattice types of bustamite and clinopyroxene, the dislocation mechanism for the in-

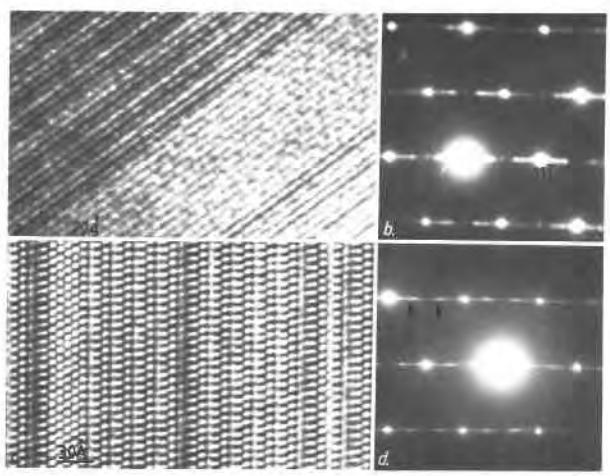

Fig. 7. Stacking disorder in clinopyroxene parallel to {11$\bar{1}$} owing to partial inversion to pyroxenoid. (a) Natural johannsenite. (b) Selected-area electron-diffraction pattern of this material after annealing in Mn solution, and (c) the corresponding image. (d) Selected-area electron-diffraction pattern from a similar specimen annealed in a Ca solution. Note the predominance of wollastonite diffraction maxima (arrowed) over those from other pyroxenoids.

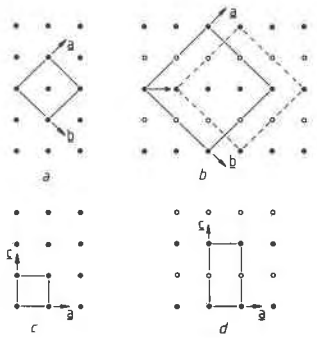

Fig. 8. Lattice sections perpendicular to the chain directions of (a) wollastonite and (b) bustamite in the cell setting of Koto et al. (1976). The horizontal arrow indicates the relative offset of the two *F*-lattices. (c and d) The same lattices with the cell setting of Peacor and Prewitt (1963). The open circles represent lattice points displaced by one-half of the lattice repeat perpendicular to the section relative to those represented by filled circles.

version of johannsenite to bustamite proposed by Angel et al. (1984) necessarily consists of two stages. The first stage is the creation of a wollastonite intermediate phase by the passage of line defects, with $\mathbf{b} = \frac{1}{4}\langle 23\bar{1}\rangle$, through the structure on the $\{11\bar{1}\}$ planes of the clinopyroxene as for the clinopyroxene-to-pyroxenoid ($I \rightarrow C$) transformations described above, followed by the inversion of this intermediate to bustamite. The inversion of pyroxenoid to bustamite would follow a similar mechanism; first, the creation of the wollastonite intermediate by the mechanism for pyroxenoid-to-pyroxenoid ($C \rightarrow C$) inversions, followed by inversion to bustamite. In the reverse direction the transformations require the inversion of bustamite to wollastonite as a first stage, followed by transformation to the product structure. Thus both types of inversion mechanism require the existence of an intermediate phase with the wollastonite structure during inversions between bustamite and either clinopyroxene or pyroxenoids.

Wollastonite and bustamite

It is clear from Figure 1 that although the individual tetrahedral chains in bustamite have the same configuration as those in wollastonite, their relative positions even in a single (100) layer are different. Figures 8a and 8b compare the lattices of wollastonite and bustamite in projection down the chain-extension direction. This shows that if the cell setting used for pyroxenoids is applied to bustamite, the lattice type is nonconventional. Koto et al. (1976) described it as an interleaved complex of two *F*-lattices with a relative displacement of the origins of $\frac{1}{4}(a + b)$. Although such a cell has advantages in comparing bustamite with the pyroxenoids, it is inconvenient to use, so although the classification of the transformations involving bustamite will retain the term "*F*-complex," an alternative cell will be used to discuss structural details of the transformation.

This simpler cell setting for wollastonite and bustamite

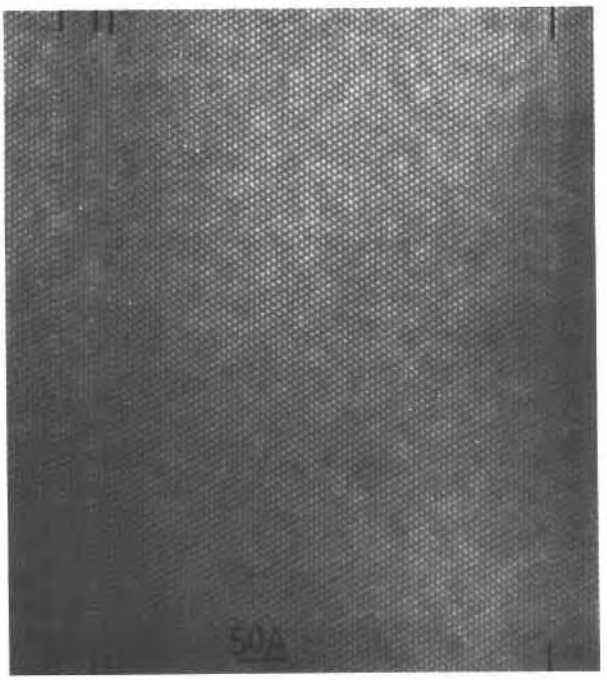

Fig. 9. Faults in a bustamite sample annealed in the stability field of wollastonite. The faults lie on the (102) planes of bustamite and have a fault vector of ½[010].

was introduced by Peacor and Prewitt (1963) and is illustrated in Figures 8c and 8d. The wollastonite cell is now primitive, while bustamite has an *A*-face-centered cell with a *c* parameter double that of wollastonite. It is now clear that the bustamite structure may be derived from that of wollastonite by the translation of alternate (001) layers by ½[010], one half of the chain-repeat distance along the chains. This relationship led Angel (1985) to propose that wollastonite and bustamite were two members of a series of polytypes based on the stacking of prismatic structural units along the **a** and **c** axes of wollastonite. Polytypic stacking variation along **a** is well known in wollastonite, and Angel (1985) found intergrowths of wollastonite and bustamite with (001) common to both phases. Transformations between these polytypes proceed by the passage of ½[010] line defects on $(h0l)$ planes; in Angel (1985) it was noted that, because of the pseudomonoclinic symmetry of the structures, glide of ½[010] defects on (101) of wollastonite and (102) of bustamite would be an alternative to glide on (001) and would also generate the other structure. Such defects were observed in an initially fault-free Fe-rich bustamite that was annealed in the stability field of wollastonite (Fig. 9). These isolated (102) faults are the beginning of the inversion to wollastonite, since in the region of a fault the relative positions of the tetrahedral chains is that of the wollastonite structure.

The structural reason for the transformation between wollastonite and bustamite proceeding by shear on the (102) planes of bustamite, or (101) of wollastonite, is quite

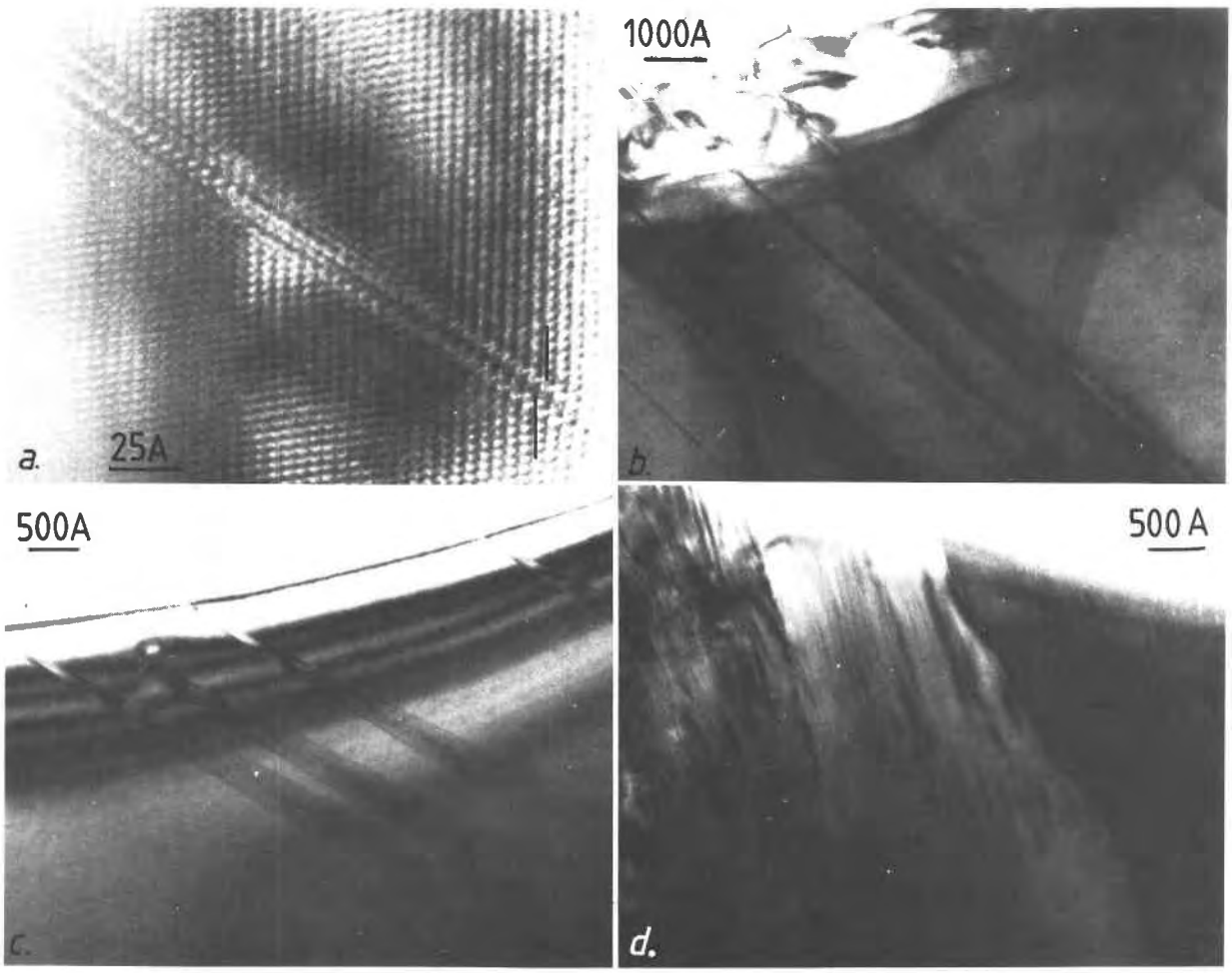

Fig. 10. (a) High-resolution micrograph of a wollastonite lamella within a clinopyroxene matrix, viewed down $[1\bar{1}0]$ of the clinopyroxene. The offset of the (110) fringes across the fault is indicated. (b) Several wollastonite lamellae parallel to a single $\{11\bar{1}\}$ plane of a clinopyroxene grain. (c) Inclined $\{11\bar{1}\}$ lamellae of wollastonite in a clinopyroxene grain and (d) subgrains of polytypically disordered bustamite in the same grain. The bustamite is oriented with [031] approximately parallel to the electron beam, the subgrains having mutual misorientations of up to 10°.

clear. In both structures these are the closest-packed planes and will thus be far more favorable for the passage of dislocations than the (001) planes, which are the slip planes suggested by simple comparison of the two stacking sequences. The observation of such faults in bustamite annealed in the stability fields of clinopyroxene or pyroxenoid is therefore interpreted as the beginning of the formation of a wollastonite-like structure as an intermediate step in the transformation from bustamite to clinopyroxene or pyroxenoid. It is to prove the existence of such an intermediate structure that the following observations are presented.

Clinopyroxene-bustamite ($I \rightarrow F$-complex)

For the study of the inversion of clinopyroxene to bustamite, a number of annealing experiments were carried out using natural johannsenite almost completely free of stacking faults. The few found were parallel to $\{11\bar{1}\}$ and consisted of short sequences of longer chain periodicities of disordered pyroxenoids (see Fig. 7a). The observations made on the products of a series of isothermal annealing of this material at 900°C (under Ar to prevent oxidation) are now presented.

The first stage in the inversion is the appearance of isolated faults parallel to the $\{11\bar{1}\}$ planes of johannsenite, as predicted by the inversion mechanism. These faults commonly run across the width of the flakes produced by crushing the sample for HRTEM for distances of several thousand ångströms. However, they are not usually single lamella of wollastonite; for example the fault in Figure 10a appears to be 28 Å wide, corresponding to the length of four chain-repeat units of a dreierketten single-chain silicate. In view of the difficulties in interpreting image contrast around faults, it would be wrong to conclude that this was indeed a lamella of four chain-repeat units of wollastonite without further evidence. In this case the

evidence is provided by the displacement across the fault of the lattice fringes of the clinopyroxene matrix. These displacements can be shown to be those that would be produced by the introduction of four wollastonite-like chain units into each chain, or overall by the introduction of four $\frac{1}{4}\langle 2\bar{3}\bar{1}\rangle$ shears into the structure.

In specimens that have undergone annealing for longer periods of time, these $\{11\bar{1}\}$ lamellae become more numerous. As seen in Figure 10b, all of the faults within a single grain lie parallel to one single $\{11\bar{1}\}$ plane of the clinopyroxene, rather than on both of the symmetry-related planes, a phenomenon first noted by Veblen (1985) in johannsenite being replaced by rhodonite and pyroxmangite. Such orientational selectivity must be due to the loss of the symmetry elements in the point group of the clinopyroxene which relate the $\{11\bar{1}\}$ planes to one another. This could occur throughout an entire grain of the clinopyroxene, which thereby makes growth processes nonequivalent on the two previously symmetrically equivalent planes, or it may occur at the point of nucleation of the line defects that give rise to the faults. In this case the most likely cause of this orientational selectivity is a phenomenon Veblen (1985) termed "templating." In a polycrystalline specimen one of the adjacent grains may, because of the relative orientation of the two grains, create a grain-boundary environment that favors fault nucleation on just one of a set of symmetry-related planes. Templating from adjacent grains is the favored explanation in this case because orientational selectivity is observed in the inversion to bustamite of polycrystalline johannsenite, whereas in their single-crystal experiments where the only "neighboring grains" were small quantities of surface oxides, Morimoto et al. (1966) found both possible orientations of bustamite inverted from johannsenite.

The need for cation synchroshear and relaxation of the structure created by the passage of a single line defect appears to favor the formation of lamellae with widths corresponding to a few chain repeats of wollastonite, rather than single faults. These multiple width faults will develop because the existence of the initial single fault will create a favorable environment for the nucleation of subsequent line defects. However, because wide wollastonite lamellae are not found, there must be a critical width beyond which it is unfavorable for the lamellae to grow by further passage of line defects.

Figure 10c shows a set of $\{11\bar{1}\}$ faults in a thinned specimen of johannsenite; a few thousand ångströms away the same original grain of clinopyroxene has inverted to bustamite (Fig. 10d). The bustamite has formed as subgrains that show relative misorientations of up to 10°. Each subgrain shows extensive polytypic stacking disorder on (100), which is eliminated during further annealing by the passage of further line defects through the structure as described by Angel (1985). These observations indicate that there then follows a period of rapid growth of the wollastonite nucleated on the lamellae, together with an almost simultaneous inversion to bustamite. That this inversion is rapid is hardly surprising when one recalls that a wollastonite structure with the johannsenite composition (ideally $CaMnSi_2O_6$) will be highly thermodynamically unstable with respect to bustamite, owing to the presence of the relatively small Mn cation. The slow rate of nucleation and growth of the lamellae may also be related to this instability, or alternatively to the need to diffuse Mn away from, and Ca to, the lamellae. A further limitation on the coherent growth of the lamellae within the clinopyroxene matrix is the volume difference between the two phases, and the relief of the strains introduced by the volume increase on inversion may account for the relative misorientations of the subgrains seen in Figure 10d.

Samples of Ca-rich bustamites from Broken Hill, New South Wales, Australia, provided an opportunity to study the initial stages of the reverse transformation, from bustamite to clinopyroxene. These bustamites have exsolved clinopyroxene by a mechanism that involves solution and reprecipitation via fluid inclusions (Wilkins and Sverjensky, 1977); HRTEM shows that the bustamite matrix has numerous faults parallel to the (102) planes. Figure 11a clearly shows that these (102) faults have an associated displacement vector of $\frac{1}{2}[010]$, and low-resolution images (Fig. 11b) indicate that they are produced by the passage of dislocations through the bustamite matrix. The presence of (102) faults, which are far more common in these than in any other natural samples studied, appears to be related to their thermal history. Experimental annealing of these bustamites increased the fault density to the point where streaking was apparent parallel to the (102) plane normal on the k-odd rows of electron-diffraction patterns (Fig. 11c). The faults therefore represent the first stage of the *solid state* mechanism of the exsolution of clinopyroxene from bustamite, being the creation of the wollastonite-like intermediate structure.

Pyroxenoid-bustamite ($C \rightarrow F$-complex)

Apart from the special case of the transformation between wollastonite and bustamite, the only other transformation of this type that occurs is that between rhodonite and bustamite. The inversion of rhodonite to bustamite is extremely rare in natural material, the only evidence for this being a few occurrences of a two-rhodonite assemblage described by Abrecht et al. (1978). In natural samples the transformation occurs far more commonly in the opposite direction as the result of metasomatic alteration of bustamite during which Ca in the structure is replaced by Mn, and more rarely bustamite may unmix at low temperatures into an assemblage of clinopyroxene plus rhodonite (Abrecht et al., 1978). However, the easiest way to study the transformation experimentally is to invert rhodonites with compositions close to the Ca-rich limit of its stability field by annealing at temperatures above the miscibility gap between the two phases (Abrecht and Peters, 1980). Such experiments have been carried out twice before in order to study the transformation by X-ray diffraction techniques and have been repeated

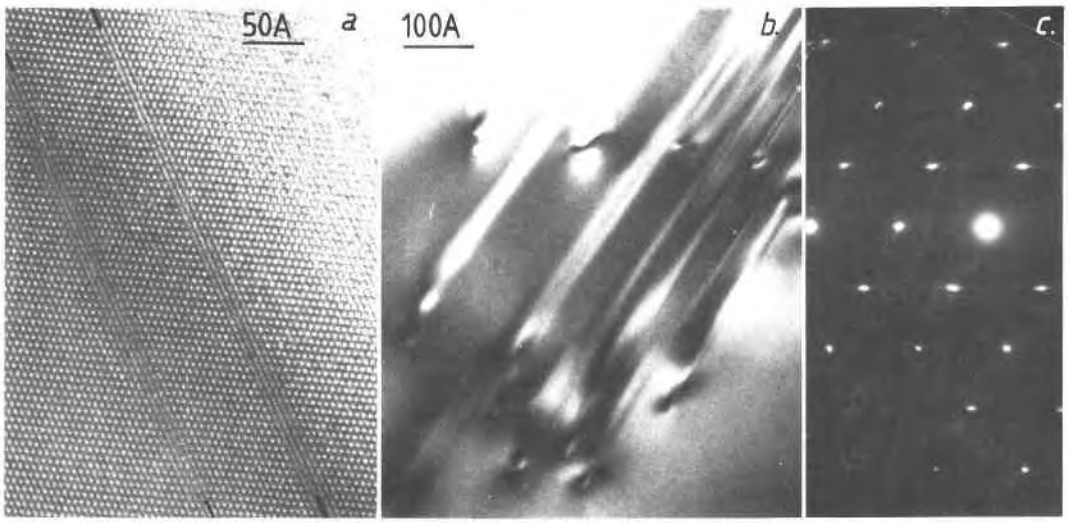

Fig. 11. (a) High-resolution micrograph of two (102) faults in a bustamite sample that has exsolved clinopyroxene and (b) a similar set of faults at lower resolution, with terminating dislocations. (c) Selected-area electron-diffraction pattern of a [21$\bar{1}$] section of a bustamite heated in the stability field of clinopyroxene. Note the streaking of the k-odd layers parallel to $\mathbf{t}^*$ (102).

here in order to study the transformation mechanism by HRTEM.

The study by Dent-Glasser and Glasser (1961) and the interpretation of their results by Morimoto et al. (1966) have been shown to be mistaken, because of the conclusion of Dent-Glasser and Glasser (1961) that the inversion product was wollastonite rather than bustamite. Yamanaka and Takéuchi (1981) also studied this inversion by heating natural rhodonite, but their primary aim was to investigate the structure of the Mn-rich bustamite produced by the inversion. Unfortunately they did not report the orientation of the product bustamite relative to the rhodonite, but did note that the morphologies of the product compared to that of the starting material suggested that an oriented transformation had taken place. Yamanaka and Takéuchi (1981) proposed an inversion mechanism of cation movement within the (100) planes similar to that proposed by Morimoto et al. (1966), but as in that paper the figures of Yamanaka and Takéuchi (1981) are of wollastonite rather than bustamite.

Similar annealing experiments were carried out in order to study the inversion by HRTEM. The material used for these experiments was a well-crystallized natural rhodonite that HRTEM showed to be free of chain-periodicity faults, but that did contain a few (100) twins. A series of annealing runs was carried out on this material, under Ar to prevent oxidation, at temperatures believed to be within the bustamite stability field. The first stage of the inversion is the creation of chain-periodicity faults in rhodonite that consist of three tetrahedra, i.e., wollastonite-like W modules. Figure 12 shows a single chain-periodicity fault in a specimen slightly inclined from the [110] axis, so that the fault lying parallel to (001) is slightly inclined. Unfortunately no partially formed chain-periodicity faults were observed in these samples so the defects that generated them can only be assumed to be identical to those involved in the pyroxenoid-to-pyroxenoid inversions. However, it should be noted that a single fault such as this cannot be produced by a purely diffusive mechanism because the number of tetrahedra in each chain has been increased within the stacking fault, whereas this is possible by a shear-type mechanism. In longer annealing runs and those at higher temperatures, the quantity of bustamite is greater, but no increase in the density of faults in the residual rhodonite grains is observed. From this it may be concluded that, as in the transformation from clinopyroxene to bustamite, the rate-determining step is the formation of narrow lamellae of wollastonite intermediate within the host phase. Once a small critical volume of the intermediate structure has been formed, it acts as a nucleus for the rapid inversion of the remaining rhodonite matrix to bustamite.

Bustamites from the bustamite-rhodonite suite described by Abrecht et al. (1978) were examined by HRTEM for evidence of the solid-state inversion mechanism of bustamite to rhodonite, or of the unmixing of bustamite to rhodonite plus clinopyroxene. In [2$\bar{1}\bar{1}$] sections of the bustamite coherent lamellae were found that lie parallel to the (102) planes of the matrix (Fig. 13a). The associated selected-area electron-diffraction pattern (Fig. 13b) shows maxima corresponding to bustamite, together with streaking parallel to the (102) plane normals on the k-odd rows, indicating random ½[010] displacements in the structure. In addition there are also weak maxima on these k-odd rows that cannot be attributed to bustamite, even in twinned orientations, but which are indexable in terms of a wollastonite unit cell (Fig. 13c). The lamellae are therefore wollastonite oriented with (101) parallel to (102) of the bustamite matrix, i.e. with the closest-packed planes of the two structures parallel. Note that the relative ori-

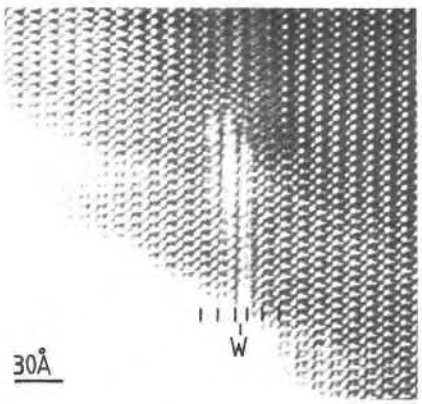

Fig. 12. A single wollastonite-like chain-periodicity fault (W) parallel to (001) in a rhodonite specimen slightly inclined from [110].

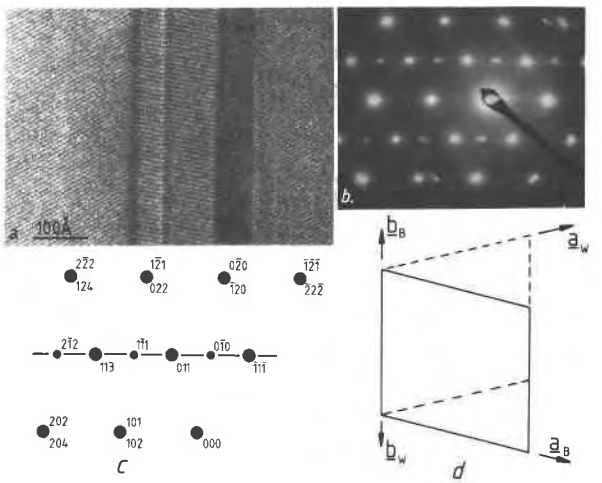

Fig. 13. (a) Wollastonite lamellae lying on the (102) planes of bustamite. (b) Selected-area electron-diffraction pattern of the specimen in (a) and (c) the indexing of this pattern. Upper indices correspond to wollastonite, lower ones to bustamite. (d) The relative orientations of the wollastonite and bustamite in real space in projection on (001).

entation is such that the wollastonite lamellae are in a twin orientation with respect to a wollastonite structure with the same stacking sequence along [100] as the bustamite matrix. In the **T,G** stacking vector notation often used to describe the wollastonite polytypes (Henmi et al., 1978), and which was extended to bustamite by Angel (1985), a ⟨**T**⟩ polytype of bustamite has (102) lamellae consisting of the ⟨**G**⟩ polytype of wollastonite. As a consequence of this twin relation, the **b** axis of the product wollastonite is parallel to $-\mathbf{b}$ of the matrix bustamite (Fig. 13d).

Discussion

In the analysis of possible mechanisms for the transformations involving the bustamite structure, the existence of an intermediate phase was postulated for structural reasons. However, the need for an intermediate structure can also be interpreted in kinetic terms. If the transformation from bustamite to either clinopyroxene or rhodonite were to be carried out by a single-step mechanism in the solid state, then this step would have to be the direct nucleation and growth of the new phase within the bustamite matrix. The different arrangement of the tetrahedral chains within the structures would result in an incoherent, or at best semicoherent, interface between the matrix and the nuclei. This in turn would lead to a high activation energy for the formation of such nuclei and thus a low overall rate for the transformation. By contrast the two-step mechanism described in this paper has much lower activation barriers and hence results in a faster rate of transformation. In forming the intermediate structure in a bustamite matrix, the first-neighbor coordinations of all the atoms remain essentially the same, with only second- and higher-neighbor coordinations being changed. The interface between wollastonite lamellae and bustamite matrix is therefore fully coherent, and the creation of this surface does not make any significant contribution to the activation energy of the transformation. Similarly, the second stage of inversion from intermediate to product phase may proceed in a fully coherent manner. This is also the first stage of the reverse transformation (i.e., to bustamite) in which coherent lamellae of wollastonite are formed within either clinopyroxene (Fig. 8) or rhodonite (Fig. 12). The formation of the wollastonite intermediate is therefore an example of the operation of the Ostwald step rule: In any phase transformation or reaction the kinetically most favorable sequence of structures will form, rather than those involving the greatest possible reduction in free energy. In the case of solid-state transformations, this is equivalent to the statement that transformations proceed via the structures that are most easily formed within the matrix of the starting material. Quite clearly this principle could be employed to suggest possible intermediate phases in other mineral transformations.

Conclusions

In this paper the possible transformations between the single-chain silicates in the (Ca,Mn,Fe,Mg)SiO_3 system have been distinguished by the change in lattice type accompanying each transformation. This change corresponds to the re-arrangement of the main structural component of these structures, the silicate chains. The observations made by HRTEM show that the transformations classified as $C \rightarrow C$ and $I \rightarrow C$ (pyroxenoid-pyroxenoid and clinopyroxene-pyroxenoid) proceed by the passage of line defects through the structure of the starting material to create the product phase. When a similar mechanism was considered for the two transformations involving the bustamite structure, it was shown that a single-step mechanism of this kind was not capable of reproducing the required lattice type, i.e., the correct distribution of the silicate chains. Careful re-examination of the alternative diffusive topotactic mechanisms previously proposed for these transformations (Morimoto et

al., 1966) showed that these too create the wollastonite structure rather than that of bustamite. Both of these types of mechanism were shown to therefore require an intermediate phase in order to carry out the transformations. This phase was confirmed to be wollastonite by HRTEM observations. Its formation can be interpreted as a consequence of the Ostwald step rule, which indicates that kinetic factors may be important in determining the mechanism of these transformations.

This study has also demonstrated the difficulties involved in characterizing solid-state transformation mechanisms in minerals, even with the use of electron microscopy. These problems mainly arise from the transient nature of the partially transformed states and the need to distinguish such microstructures from other artifacts, such as growth faults in the starting material and faults induced by specimen preparation. The latter two problems were avoided in this study by the careful characterization of starting materials by HRTEM and by preparing specimens for electron microscopy by both crushing and ion-beam thinning. It is unlikely that these two very different preparation methods would introduce the same types of faults into the specimens, and comparison of observations made on samples prepared by both methods did allow some specific artifacts of the crushing of samples to be identified as such.

However, the assumption remains that the quenched-in faults observed in samples recovered from a series of isothermal annealing experiments do represent the complete sequence of transformation states. Indeed this study provides examples in that although the wollastonite-like intermediate structure has been observed, the mechanism by which it is transformed to and from clinopyroxene and rhodonite was not directly observed. Rather it was deduced that these transitions were likely to proceed by the propagation of line defects. Similarly, because of the apparently rapid transformation rates, no transition was observed between the microstructures shown in Figures 10c and 10d. Until it is possible to study such transformations in situ in the electron microscope at high resolution, the results of a study such as this may be subject to reinterpretation.

Acknowledgments

Thanks are due to Dr. Andrew Putnis for his supervision of this project, and to him, Dr. Mike Bown, and Dr. David Price for their helpful comments on draft versions of this paper. The review by Dr. Ian McKinnon contributed much to the organization of the material presented here. Natural specimens were kindly donated by Professor T. G. Vallance of the University of Sydney Geology Department, Dr. J. Abrecht of the Mineralogical Institute of Basel University, and Dr. G. Chinner, curator of the Harker collection of the Earth Sciences Department, University of Cambridge. This work was carried out with the support of a research studentship from the Natural Environment Research Council of Great Britain.

References

Abrecht, J., and Peters, Tj. (1980) The miscibility gap between rhodonite and bustamite along the join $MnSiO_3$-$Ca_{0.6}Mn_{0.4}SiO_3$. Contributions to Mineralogy and Petrology, 74, 261–269.

Abrecht, J., Peters, Tj., and Sommerauer, J. (1978) Manganiferous mineral assemblages of Ravinella di Sotto, Valle Strona, Italy. Memorie di Scienze Geologische, 33, 215–221.

Aikawa, N. (1979) Oriented intergrowth of rhodonite and pyroxmangite and their transformation mechanism. Mineralogical Journal of Japan, 9, 255–269.

——— (1984) Lamellar structure of rhodonite and pyroxmangite intergrowths. American Mineralogist, 69, 270–276.

Amelinckx, S., and Van Landuyt, J. (1976) Contrast effects at planar interfaces. In H.-R. Wenk, Ed. Electron microscopy in mineralogy. 68–112. Springer-Verlag, Berlin.

Angel, R.J. (1984) The determination of the johannsenite-bustamite equilibrium inversion boundary. Contributions to Mineralogy and Petrology, 85, 272–278.

——— (1985) Structural variation in wollastonite and bustamite. Mineralogical Magazine, 49, 37–48.

Angel, R.J., Price, G.D., and Putnis, A. (1984) A mechanism for pyroxene-pyroxenoid and pyroxenoid-pyroxenoid transformations. Physics and Chemistry of Minerals, 10, 236–243.

Czank, M., and Liebau, F. (1980) Periodicity faults in chain silicates: A new type of planar lattice fault observed with HREM. Physics and Chemistry of Minerals, 6, 85–93.

Czank, M., and Simons, B. (1983) High resolution microscope studies on ferrosilite III. Physics and Chemistry of Minerals, 9, 229–234.

Dent-Glasser, L.S., and Glasser, F.P. (1961) Silicate transformations: Rhodonite-wollastonite. Acta Crystallographica, 14, 818–822.

Henmi, C., Kusachi, I., Kawahara, A., and Henmi, K. (1978) 7T wollastonite from Fuka, Okayama Prefecture. Mineralogical Journal of Japan, 9, 169–181.

Jefferson, D.A., and Pugh, N.J. (1981) The ultrastructure of pyroxenoid chain silicates, III. Intersecting defects in a synthetic iron-manganese pyroxenoid. Acta Crystallographica, A37, 281–286.

Jefferson, D.A., Pugh, N.J., Alario-Franco, M., Mallinson, L.G., Millward, G.R., and Thomas, J.M. (1980) Ultrastructure of pyroxenoid chain silicates, I. Variation of chain configuration in rhodonite. Acta Crystallographica, A36, 1058–1065.

Koto, K., Morimoto, N., and Narita, H. (1976) Crystallographic relationships of the pyroxenes and pyroxenoids. Japanese Association of Mineralogists, Petrologists and Economic Geologists Journal, 71, 248–254.

Kronberg, M.L. (1957) Plastic deformation of single crystals of sapphire: Basal slip and twinning. Acta Metallographica, 5, 507–524.

Lacam, A., Madon, M., and Poirier, J.P. (1980) Olivine glass and spinel formed in a laser heated, diamond anvil high pressure cell: An investigation by transmission electron microscopy. Nature, 288, 155–157.

Morimoto, N., Koto, K., and Shinohara, T. (1966) Oriented transformation of johannsenite to bustamite. Mineralogical Journal of Japan, 5, 44–64.

O'Keefe, M.A., and Buseck, P.R. (1979) Computation of high resolution TEM images of minerals. American Crystallographic Association Transactions, 15, 27–46.

Pannhorst, W. (1979) Structural relationships between pyroxenes. Neues Jahrbuch für Mineralogie Abhandlungen, 135, 1–17.

Peacor, D.R., and Prewitt, C.T. (1963) Comparison of the crystal structures of bustamite and wollastonite. American Mineralogist, 48, 588–596.

Poirier, J.P. (1981) On the kinetics of the olivine-spinel transition. Physics of the Earth and Planetary Interiors, 26, 179–187.

Prewitt, C.T., and Peacor, D.R. (1964) Crystal chemistry of the pyroxenes and pyroxenoids. American Mineralogist, 49, 1527–1542.

Price, G.D., Putnis, A., and Smith, D.G.W. (1982) A spinel to β-phase transformation mechanism in $(Mg,Fe)_2SiO_4$. Nature, 296, 729–731.

Putnis, A., and Price, G.D. (1979) High pressure $(Mg,Fe)_2SiO_4$ phases in the Tenham chondritic meteorite. Nature, 280, 217–218.

Ried, H. (1984) Intergrowth of pyroxene and pyroxenoid: Chain periodicity faults in pyroxene. Physics and Chemistry of Minerals, 10, 230–235.

Ried, H., and Korekawa, M. (1980) Transmission electron microscopy of synthetic and natural funferketten and siebenerketten pyroxenoids. Physics and Chemistry of Minerals, 5, 351–365.

Simons, B., and Woermann, E. (1982) Pyroxene-pyroxenoid transformations under high pressure. In W. Schreyer, Ed. High pressure researches in geoscience, 529–536. E. Schweizerbart'sche Verlagbuchhandlung, Stuttgart.

Taylor, H.F.W. (1960) Aspects of the crystal structures of calcium silicates and aluminates. Journal of Applied Chemistry, 10, 317–323.

Veblen, D.R. (1985) TEM study of a pyroxene-to-pyroxenoid reaction. American Mineralogist, 70, 885–901.

Wilkins, R.W.T., and Sverjensky, D.A. (1977) The role of fluid inclusions in the exsolution of clinopyroxene in bustamite from Broken Hill, New South Wales, Australia. American Mineralogist, 62, 465–474.

Yamanaka, T., and Takéuchi, Y. (1981) X-ray study of the rhodonite-bustamite transformation. Zeitshrift für Kristallographie, 157, 131–145.

MANUSCRIPT RECEIVED SEPTEMBER 20, 1985
MANUSCRIPT ACCEPTED JULY 8, 1986